Parametric Study of the Effect of Wrinkle Features on The Strength of a Tapered Wind Turbine Blade Sub-structure

J. J. Bender[1,*], S. R. Hallett[2] and E. Lindgaard[1]
[1]Department of Materials and Production, Aalborg University, Fibigerstraede 16, 9220 Aalborg East, Denmark
[2]Bristol Composites Institute (ACCIS), University of Bristol, Queens Building, Bristol BS8 1TR, United Kingdom
[*] Corresponding author email address: bender@mp.aau.dk

Abstract
Out of plane wrinkle defects are a major cause of strength reduction in structural composites. Therefore, this paper presents the numerical modelling of a wind turbine blade sub-structure with a tapered beam and a wrinkle. The model is validated against preliminary static tensile tests of a sub-structure without a wrinkle. There is a very good correlation between the predicted and experimentally obtained load at final delamination. A parametric study is then performed using the validated model to determine which wrinkle features are the most important to measure and include when determining the strength of a wrinkled wind turbine blade sub-structure. From the study, it is concluded that the maximum wrinkle angle is the most important feature, but the depth and wash out degree are also important under the right conditions.

Keywords: *Sub-structure, Wrinkle defect, Tapered beam, Cohesive Zone Modelling, Delamination*

1. Introduction

Wind turbine blades (WTBs) are getting bigger, meaning the moulds are getting bigger and more expensive as well. Therefore, each blade is becoming more valuable, and discarding a blade due to a defect is expensive [1]. This means that blades that have a severe defect need to be repaired, which is still an expensive procedure due to the labour intensive nature of the repair [1]. One of the typical types of defects are wrinkle defects in areas of thickness reduction close to the root where even small wrinkles can initiate severe damage due to the high loading. The large thickness and rapid change in thickness in the root cause WTB manufacturers to consider using pre-fabricated reinforcements such as pultruded tapered beams[1] to reduce production time and avoid many ply drops in close proximity to each other. When these pre-cured pultruded beams are included in the Vacuum Assisted Resin Transfer Moulding (VARTM) process of a WTB there is an increased probability of causing wrinkles in the root. This is due to the significant change in stiffness from the pultruded beam to the dry uncured fibre mats, which can lead to wrinkling when the vacuum is applied.

However, it is unclear when the severity of a wrinkle requires a repair, and when it is insignificant, and will not affect the lifetime of the blade. The effect of wrinkles on the tensile and compressive strength of laminates has been investigated in the literature. In [2] experiments and simulations on quasi-isotropic Carbon Fibre Reinforced Polymers (CFRP) sandwich panels were conducted and a reduction of up to 55% in compressive strength was reported when all layers were affected by a wrinkle with an angle between the load direction and maximum slope of the wrinkle of up to $\approx 73^\circ$. This angle is henceforth referred to as the maximum wrinkle angle. In [3] a multi-directional CFRP laminate was tested in compression, where smaller maximum wrinkle angles of up to 12° were tested. The reduction in compressive strength was $\approx$30%, where most of the embedded layers were affected by the wrinkle. The failure was a mixture of fibre failure and delamination with fibre breakage occurring first. The same authors conducted experiments in tension as well in [4], where a reduction of $\approx$20% in tensile strength was reported for a maximum wrinkle angle of 12°. Again, most of the embedded layers were affected by the wrinkle, and the primary damage mode was delamination.

Experiments have been conducted on Glass Fibre Reinforced Polymer (GFRP) as well. In [5] a reduction of $\approx$25% in compressive strength was reported at wrinkle angles of $\approx 50^\circ$ for a sandwich panel with a wrinkle through the entire thickness of one face sheet. The face sheets constituted of primarily unidirectional (UD) layers and the primary failure mode was delamination. In [6] a reduction in tensile strength of $\approx$22% was reported for a maximum wrinkle angle of 12° for a pure 0° lay-up. The wrinkle affected all layers and the primary failure mode was delamination. In [7] pure UD GFRP laminates were tested, where half the thickness of the laminate was wrinkled at an angle of 29° with a reduction in tensile strength of 14%. The failure modes were delamination and fibre failure.
A recent parametric study of the importance of wrinkle geometry [8] showed that the most important wrinkle parameter w.r.t. knock-down of compressive strength is the maximum wrinkle angle followed by the length of the wrinkle. The maximum wrinkle angle caused a 40% increased knock-down when the angle was increased from 4° - 28°. There was also a significant dependence on the extent of the wrinkle through the thickness.

To the knowledge of the authors, no research has been done on Fibre Reinforced Polymer (FRP) laminates produced with VARTM where tapered pultruded beams are included in the moulding process. Most research has focused on ply-drops due to ply terminations and the associated failure mechanisms. It is reported in [9] that the failure sequence of a ply-drop in a GFRP laminate in tension starts with matrix cracks at the termination of the ply on the surface normal to the load direction. This leads to delamination growth on top and bottom of the dropped ply. Followed by matrix cracking in the outer layers, and delamination in the thin part. Lastly, the delaminations grow in both directions causing final failure. For the case of a pultruded tapered beam the discrete termination is less pronounced meaning that the first matrix cracks are less likely to occur. But there are also many similarities, meaning that the failure sequence is most likely comparable.

In [10] Finite element analyses were conducted on ply-drops in a CFRP laminate with different taper angles. It was reported that for shallow taper angles (7°) the material of the area in front of the terminated ply had a big influence on the damage progression. In [10] the area in front of the terminated ply was either modelled as a resin pocket, or was not modelled at all, meaning the resin pocket had the same characteristics as air. With resin, delaminations developed in the thick direction, whereas with no resin, a delamination developed in the thin direction. With a pultruded tapered beam the material is neither resin nor air, and therefore the damage progression could be different.

One work [11] has focused on out-of-plane waviness in a tapered beam section. The work focused on multiple wrinkles found in flexbeams used for helicopter blades manufactured from GFRP. The

[1]Fiberline Composites A/S. Blade Root Reinforcements. https://fiberline.com/wind-turbine-components/blade-root-reinforcements

effect of the waves was quantified by determining the reduction in fatigue life due to the wrinkles. The flexbeams were loaded with a static tensile force and a cyclic transverse load causing cracks at the wrinkles leading to delamination growth in both directions. The authors concluded that no wrinkles were allowed in the thin part of the flexbeam because the fatigue life would be reduced by it. However, small wrinkles (1.5° - 5°) in the thick part were allowed. The authors based their conclusions purely on the interlaminar normal stress and neglecting interlaminar shear stresses.

From the above it is apparent that the damage progression for tapered composites and composites with wrinkles is complex. The primary damage mechanisms in the above-mentioned works are delaminations. Therefore, in this work, Cohesive Zone (CZ) elements are used in a Finite Element (FE) framework to model the development of delaminations from initiation to propagation. Different wrinkle configurations are simulated to determine the interaction between the wrinkle and the tapered beam. The location of the wrinkle w.r.t. the tip of the tapered beam, the maximum angle of the wrinkle, the depth of the wrinkle, and the wrinkle angle through the thickness of the beam, which is controlled by the wash out degree, are the varied parameters in a parametric study. This study can be used to identify which parameters are important to focus on when modelling wrinkles e.g. found in manufactured WTBs.

In section 2 the different scales used in this work are presented along with a presentation of the origin of the tested sub-structure. In section 3 the finite element modelling is described along with the methodology for modelling wrinkles and cohesive elements. In section 4 the numerical model is validated based on experiments. In section 5 the results of the parametric study are presented and the trends are highlighted. The results and the relevance of the average wrinkle angle are discussed in section 6. Finally, in section 7 a conclusion of the work is presented.

2. Wind Turbine Blade Scales

This work focuses on defects related to the root section of WTBs. The root of a typical WTB consists of a thick GFRP laminate and a severely tapered section. At the tip of the tapered section, there is an increased risk of wrinkle defects. As it is shown in Fig. 1 the area of interest is at a small scale compared to the entire wind turbine blade.

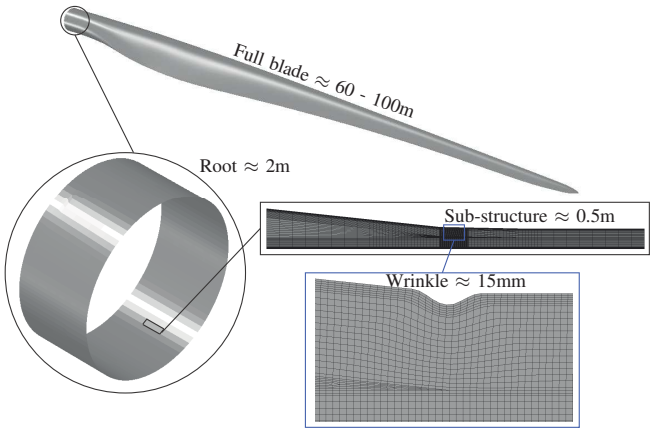

Fig. 1 Illustration of scales involved in testing Wind Turbine Blades.

Therefore, full scale testing of complete blades is overkill in this context. However, sub-structure testing with thicknesses similar to the real WTB in the area of interest is very useful to verify numerical results. The sub-structure testing can be performed at a fraction of the cost for a full scale blade test, however, testing of sub-structures is still complex and time consuming. Therefore, as few tests as possible should be performed. In this work, four sub-structures have been cut out from an actual WTB without wrinkles and tested in static tension. The results are used to validate the numerical model before the model is in turn used to analyse the effect of the interaction between the tapered beam and a wrinkle. An image of the sub-structure is shown in Fig. 2, where approximate length, width, and thickness are denoted. The lay-up consists of biaxial layers at the top and bottom, triaxial layers at the interface between the insert and the laminates and UD material in the rest with fibres in the length direction of the sub-structure. Since the sub-structures are cut from an actual blade, the lay-up is identical to the one found in actual blades. The stacking sequence is also depicted in Fig. 3.

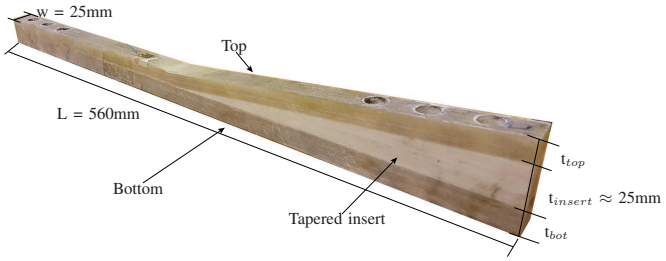

Fig. 2 Image of a tested sub-structure with length, L, width, w, and approximate thickness of the tapered insert, t_{insert}. The thickness of the bottom laminate, t_{bot}, is 10% larger than the thickness of the top laminate, t_{top}.

3. Numerical Model - Geometry and Mesh

3.1 Mesh and Lay-up

The numerical simulations are performed in ABAQUS explicit. The C3D8R solid-elements, which are 3D solid elements with 8 nodes and reduced integration, are used to model the overall geometry of the specimen. The model is made as a slice model with one element through the width of the specimen (z-direction), and movement in the z-direction is constrained on one surface normal to the z-direction. This yields a plane stress condition. The structural response and load at final delamination with this slice model is similar to that of a model with more elements in the z-direction and the same width as the actual sub-structure.

There is one element in the thickness direction of each ply and the element length in the x-direction is reduced closer to the tip of the insert with a minimum length of 1 mm as shown in Fig. 3. The element length in each of the sections is determined based on convergence studies. The length of mesh region 1 is determined based on the length of the wrinkle to ensure that the entire wrinkle is within the region with the finest mesh. The loading is applied as a prescribed displacement at the end of the model.

3.2 Cohesive Zone Modelling

COH3D8 interface-elements, which are 8 noded interface elements, are used to model the cohesive interfaces. The cohesive elements are inserted between every ply in the model in mesh region 1 and 2 with zero thickness. The initiation of damage in the cohesive elements is determined based on a quadratic relation of the onset normal- and shear-tractions as shown in the equation below.

$$\left(\frac{\sigma_n}{\sigma_n^0}\right)^2 + \left(\frac{\sigma_{s1}}{\sigma_{s1}^0}\right)^2 + \left(\frac{\sigma_{s2}}{\sigma_{s2}^0}\right)^2 = 1 \qquad (1)$$

Where σ_n is the normal traction, σ_{s1} and σ_{s2} are the shear tractions along and perpendicular to the load direction, respectively. The ^{0}

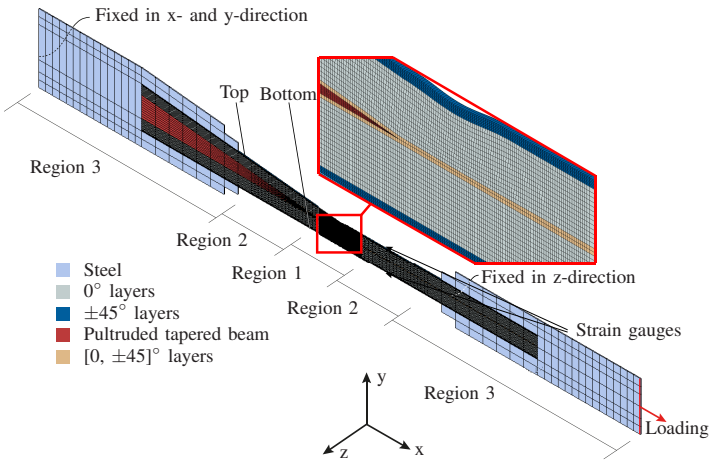

Fig. 3 Mesh of the FE model with a close-up at the wrinkle and tip of the tapered beam.

indicates the onset traction for the corresponding traction.

The damage evolution is modelled with a bilinear law using Benzeggagh-Kenane (BK) fracture interaction criterion to account for mixed-mode loading as shown in Eq. 2.

$$G_n^c + (G_s^c - G_n^c)\left(\frac{G_s + G_t}{G_n + G_s + G_t}\right)^p = G^c \tag{2}$$

Where G_n, G_s, and G_t are the energy release rates in the normal- and two shear directions, respectively. The ^{c} indicates the critical energy release rate in the given direction and ^{p} is a curve fitting parameter, which in this work is set to 1, corresponding to a linear interaction between normal- and shear-mode mixity.

The interfacial properties are reduced for the interface between the pultruded insert and the surrounding laminate by 20% for the onset tractions w.r.t. the properties of the interface between two layers in the same laminate. This reduction is based on fitting between the experimental result and the numerical model. The critical energy release rates are reduced by 28% corresponding to the reduced interfacial behaviour observed by the manufacturer. These reductions in interfacial properties indicate less fibre bridging between the insert and the surrounding laminate. No material values are reported in this work due to confidentiality with the WTB manufacturer. However, it can be reported, that the stiffness of the tapered insert is 38GPa[2], which is more than 15% lower than the stiffness of the unidirectional material.

3.3 Wrinkle Modelling

The wrinkle is included in the model by moving the existing nodes of the pristine model in the thickness direction as in Eq. 3.

$$y = y_{pri} + y_{wri} \tag{3}$$

Where y_{pri} is the y-coordinate of nodes in the pristine model w.r.t. the centre of the wrinkle, y_{wri} is the movement of the nodes in the y-direction (Fig. 3) due to the wrinkle, and y is the y-coordinate of the nodes affected by a wrinkle w.r.t. the centre of the wrinkle. The centre of the wrinkle is moved in the x-direction and the location is defined relative to the tip of the insert. The centre is kept at the surface of the model. The initial wrinkle is modelled with a sine function based on the height, a, and length of the wrinkle, L, where these are the amplitude and period, respectively. The maximum wrinkle angle can be determined based on these two parameters as in Eq. 4 [12].

$$\theta = tan^{-1}\left(\frac{\pi \cdot a}{L}\right) \tag{4}$$

The total depth of the wrinkle, $depth$, and the wash out through the thickness of the specimen, i.e. the flattening of the wrinkle, are predetermined parameters as well. The rate of wash out is determined based on the wash out power, w, meaning that a power of 1 results in a linear decrease of maximum wrinkle angle through the thickness. An increase in wash out power means that the wrinkle angle is almost constant through some of the thickness and close to the maximum depth the wrinkle angle washes out very quickly. The effect of the four parameters is illustrated in Fig. 4, and they affect the wrinkle model as in Eq. 5.

$$y_{wri} = \frac{a}{2} \cdot (1 - z^w) \cdot \left(cos\left(\frac{x \cdot \pi}{\frac{L}{2} + y_{pri}}\right) + 1\right) \tag{5}$$

Where x is the x-coordinate of nodes in the pristine model w.r.t. the centre of the wrinkle, and z is defined as $z = \frac{y_{pri}}{depth}$.

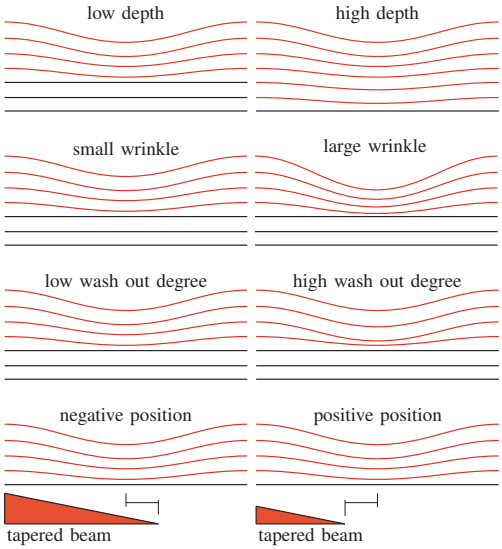

Fig. 4 Illustrations of how the four parameters affect the wrinkle shape through the thickness of the model.

3.4 Preliminary analysis of the failure initiation

Fig. 5a and 5b show the Initiation Index (II) from the failure onset criterion in Eq. 1 for the pristine model and a model with a wrinkle, respectively at similar global load level. It is shown that the II is highest at the tip of the insert for the pristine case and close to the top of the sub-structure for the wrinkled case. The simulation is linear until any of the cohesive elements is damaged, and non-linear after. Therefore, the first element with any damage is located in the region with the highest stress. It is not possible, based on the stress alone, to determine with certainty where final failure occurs, because there can be substantial non-linear behaviour. This is exemplified by Fig. 5a and 5b where there is only one area in each case with a high initiation index, II, but final failure occurs at the insert for both, which is not apparent from the stress plots. In the wrinkled case, a delamination occurs at the wrinkle first, but does not propagate, and final failure occurs later at the insert. Due to the non-linear behaviour in the wrinkled case it is not possible to determine the location or load at final failure from a pure linear static stress analysis. The final failure load and location is dependent on load redistribution due to damaged interfaces. Therefore, progressive damage modelling using

[2]Fiberline Composites A/S. Blade Root Reinforcements. https://fiberline.com/wind-turbine-components/blade-root-reinforcements

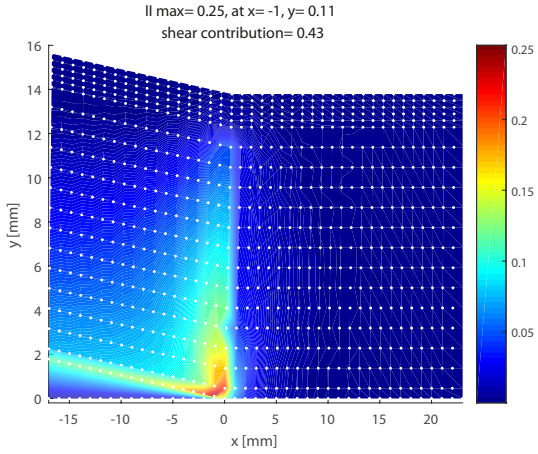

Fig. 5a II of pristine model, where the top half at the tip is shown. (White dots represent nodes in the interfaces)

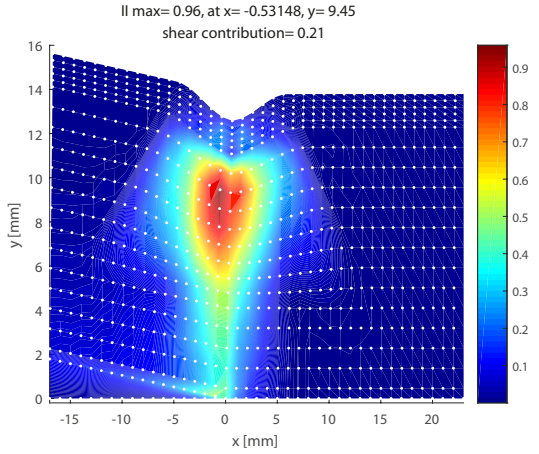

Fig. 5b II of a model with a medium wrinkle, where the top half at the tip is shown. (White dots represent nodes in the interfaces)

cohesive zone elements is necessary to conduct these analyses.

The figure for the pristine case also shows that the contribution from shear stress to the total II is close to 0.5 at the location of maximum II meaning that normal and shear stresses are almost equally important. The contribution from the shear stress is lower in the wrinkled case than in the pristine case indicating that the normal stress is more controlling for a wrinkle configuration as shown in 5b.

4. Experimental Validation of Model

The numerical model is validated by comparing the results from a simulation of the pristine sample with the results from experiments. The sub-structure was cut out from an actual WTB without a wrinkle and tested in the test rig shown in Fig. 6. To prevent an eccentric loading, the load was introduced in the centre of the cross-section of the sub-structure measured on the thin part of the sub-structure.

The sub-structure was loaded in static tension up to the point

Fig. 6 Test setup used to produce verification results.

where it lost a significant amount of load-carrying capacity due to delamination. The load at this point was then used to compare to the simulation. Furthermore, strain data was acquired during the test on top and bottom of the thin part of the sub-structure 60mm from the tip (as indicated in Fig. 3). High-speed cameras were used as well to capture the damage mode when the sub-structure lost load-carrying capacity. The validation of the FE-model is shown in Fig. 7. The strain on top and bottom of the sub-structure for simulation and experiment were similar throughout the entire static test and the load at final failure for the sub-structure with highest load was predicted with less than 1% error as well. It should be noted that the onset traction values used in the model have been fitted to minimise the difference in load at final failure. In Fig. 7 there are two small triangular shapes on the load curves. The load drop is caused by settling of the grips and the triangular shape appears because of an insignificant delay between the data from the strain gauges and the load cell.

The qualitative damage mode was similar for the simulation and

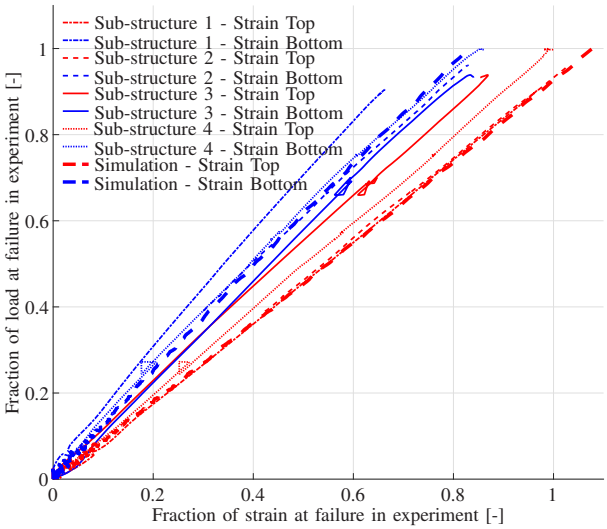

Fig. 7 Plot of the load as a function of strain on top and bottom of the non-wrinkled sub-structure during the static tensile test. All results have been normalised w.r.t. load and strain at failure in experiment for the sub-structure with highest failure load.

the experiments as well. The final delamination ran on top and bottom of the insert for the simulation and experiments as shown in Fig. 8.

The accuracy of the numerical model is hereby validated with respect to its ability to predict the correct damage mechanism, being delamination on top and bottom of the insert and the load at final

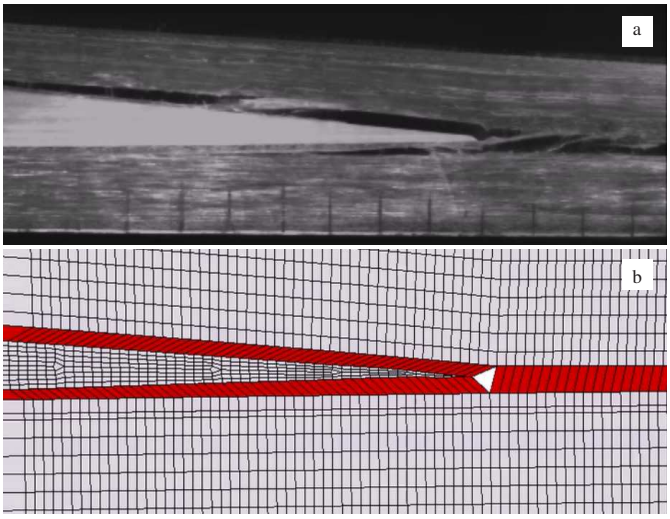

Fig. 8 Comparison of damage mode at insert tip in (a) experiments and (b) simulation, red colour indicates delamination failure of cohesive elements.

failure. Based on this, it is assumed that the model can be used to predict the behaviour of a similar sub-structure with different variations of wrinkles included. Further comparison between experiments and numerical models are shown in [13].

5. Results

The relevant parameters for the wrinkle shape have been identified and are illustrated in Fig. 4. These parameters are varied to determine the interaction between the parameters and the relation between each of the parameters and the load at final failure. By understanding the interaction between the parameters it is possible to determine if there are some cases where some of the parameters are less important and therefore not required through Non Destructive Evaluation (NDE) when evaluating the severity of a wrinkle in an actual blade.

Final failure is defined as a delamination crack spanning from a cohesive element at the centre of the sub-structure to either the area between mesh region 2 and 3 near the fixture in Fig. 3 or the area between mesh region 2 and 3 near the load introduction.

In the following section the four mentioned parameters are varied within reasonable limits of what is typically observed during the VARTM process of WTB root sections. The levels are as shown in Table 1a and 1b.

Table 1a Parameters (P) that influence the average wrinkle angle, and their levels (L).

P \ L	Small	Medium	Large
Maximum wrinkle angle [°]	12	21	29
Depth [mm]	6	10	14
Wash out degree [-]	1	3	5

Table 1b Parameter that does not influence the average wrinkle angle, and its levels.

Location
-1mm
0mm
+1mm
+2mm

The maximum wrinkle angle is chosen as 12°, 21°, and 29°. These values reflect the maximum wrinkle angles in the literature and they are representative of wrinkles found after manufacturing. The depth is chosen as 6mm, 10mm, and 14mm, corresponding to a wrinkle that straightens out very quickly through the depth, and going to a wrinkle that affects all the plies from the surface to the tip of the insert. The location of the centre of the wrinkle is chosen as -1mm, 0mm, +1mm, and +2mm w.r.t. the tip of the insert, where a negative value means that the centre of the wrinkle is on the thick part of the laminate. These locations are chosen since the centre of the wrinkle is very close to the tip of the insert for all inspected manufactured cases. The wash out degree is chosen as 1, 3, and 5, which covers the reasonable wash out shapes. It is not possible to increase the degree more than this; otherwise the deepest layers will overlap. These possible levels of the four parameters lead to 108 combinations, which have been simulated to get the interaction between all parameters.

In [14] the average wrinkle angle through the entire thickness of the specimen is used instead of the maximum wrinkle angle. A good agreement is achieved between the failure stress in compression and the average out-of-plane waviness. The average wrinkle angle is applied in this work as well, where the angle is averaged from the top surface of the sub-structure to the tip of the insert. The wrinkle angle is determined based on Eq. 4 continuously down through the thickness to the tip of the insert. This leads to the expression of the average wrinkle angle as in Eq. 6. The angle decreases through the thickness as a function of the amplitude and length of the wrinkle based on the wash out degree and the total depth of the wrinkle, as shown in Eq. 7 and 8.

$$\theta_{avg} = \frac{1}{t} \cdot \begin{cases} \int_0^t tan^{-1}\left(\frac{\pi \cdot a_y(y)}{L_y(y)}\right) dy & y \leq depth \\ 0 & y > depth \end{cases} \tag{6}$$

Where

$$a_y(y) = a \cdot \left(1 - \left(\frac{y}{depth}\right)^w\right) \tag{7}$$

$$L_y(y) = L + y \tag{8}$$

Where y is the distance in the y-direction from the centre of the wrinkle toward the insert and t is the total thickness from the top surface to the tip of the insert.

5.1 Parametric study

The results from the parametric study are shown in Fig. 10a-c, 11a-c, and 12a-c. It should be noted that the data in Fig. 10a-c is the same as in Fig. 11a-c and Fig. 12a-c, the only difference is which parameters are constant. There is a lot of information in each of the figures, therefore, Fig. 9 is introduced first, to give the reader an understanding of the generic features of the result figures. For each of the figures in the result section one parameter is constant and the other three are varied within the limits of the respective parameter. The result figures are divided in groups of three where the constant parameter is then varied from one figure to the next. There are three shaded areas in each of the figures and in each of the shaded areas a second parameter is constant. The green areas indicate the low level of the parameter, the red indicate the medium level of the parameter, and the blue indicate the high level of the parameter. There are three groups of vertically aligned data points in all of the shaded areas, and a third parameter is varied between these three groups. The group to the left indicate the low level, the central group indicate the medium level, and the right group indicate the high level of the third parameter. The vertically aligned data points in each of the groups indicate the different locations of the wrinkle w.r.t. the tip of the insert.

The wash out degree is kept constant within each of the first six figures, but varied between the figures. The depth is kept constant within each of the last three figures, but varied between them. The

depth is the same for all results within a shaded area for Fig. 10a-c, and the maximum wrinkle angle is the same for all results within a shaded area for Fig. 11a-c and 12a-c. In each of the shaded areas only the location of the centre of the wrinkle is varied along with either the maximum wrinkle angle, the depth, or the wash out degree.

The effect of the location of the wrinkle is indicated by the scatter of data points for each average wrinkle angle, meaning that data points on top of each other indicate that the location has almost no influence on the load at final failure, and a large scatter indicates a big influence of the location. The location of the wrinkle for the given data point is indicated next to it.

The sensitivity of the knock-down to the maximum wrinkle angle is indicated by the slope in Fig. 10a-c. For each of the shaded areas the points to the left have a maximum wrinkle angle of 12° and going to the right the angle increases to 21° and 29°, respectively. The sensitivity of the knock-down to the depth is indicated by the slope of each of the shaded areas in Fig. 11a-c. For each of the shaded areas the points to the left have a depth of 6mm and going to the right the depth increases to 10mm and 14mm, respectively. The sensitivity of the knock-down to the wash out degree is indicated by the slope in Fig. 12a-c. For each of the shaded areas the points to the left have a wash out degree of 1 and going to the right the degree increases to 3 and 5, respectively. The black lines in the figures indicate the slope of the average values within each of the shaded areas, and the number next to the lines indicate the slope parameter.

The wrinkle and the tip of the tapered beam both act as damage initiators in the model. The wrinkle is varied in severity in the next section, and depending on the severity of the wrinkle, final failure can be either a delamination at the insert, or a delamination between two wrinkled plies. For most cases, final failure is a delamination at the insert, where the stress concentration from the wrinkle increases the stress at the tip of the insert. Final failure occurs between two wrinkled plies in many cases for medium and large wrinkles, as indicated by the black circles in Fig. 10a-c. None of the configurations with a depth of 14mm show final failure between two wrinkled plies. It is shown that by moving the centre of the wrinkle a few millimetres w.r.t. the tip of the insert the final failure mode can change from an insert delamination to a delamination between two wrinkled plies. This results in a significant increase in the knock-down of the tensile strength. This is for example indicated in Fig. 10b, where the location can cause a change in the knock-down from 17 - 55% with a medium depth, a medium wash out degree, and a medium maximum wrinkle.

It is determined using a three-way analysis of variance (ANOVA) if the four parameters influence each other in any way. Through the ANOVA, no significant effect of the location is found and therefore this parameter is excluded from the three-way ANOVA and instead used as replicates for the other parameters. The other three parameters are significant, and the pairwise interaction between them is significant as well.

In the following sections the effect of each of the parameters and the interaction between them is determined in a qualitative manner. The slope parameters for all the grouped results are gathered in Table 2, 3, and 4.

5.2 Maximum Wrinkle Angle

A general trend for all the results is that the knock-down is increased when the maximum wrinkle angle is increased. However, it is shown in Fig. 11a that a small maximum wrinkle angle with a large depth yields a higher knock-down than a medium maximum wrinkle angle with a small depth (The points to the right in the green area have a higher knock-down than the points to the left in the red area). This is only valid when the wash out degree is equal to one, indicating that the maximum wrinkle angle is very controlling of the knock-down and only in a few cases can a small maximum wrinkle angle be more severe than a larger maximum wrinkle angle. The sensitivity of the knock-down to the maximum wrinkle angle is only slightly affected by changes in the depth and wash out degree. This is indicated by the similar slopes in Fig. 10a-c and coefficients in Table 2. This means that accurate measurements of the height and length of the wrinkle is required for accurate knock-down results independent of the depth and wash out degree of the wrinkle. However, there is one exception. Fig. 10b and 10c show that for a small depth and medium to high wash out degree there is almost no difference in knock-down for a medium and large maximum wrinkle angle. From Fig. 10a it seems that the average wrinkle angle can be used to describe the knock-down. However, when the wash out degree is increased in Fig. 10b and Fig. 10c the scatter is increased significantly and a direct relation between the average wrinkle angle and the knock-down is not possible.

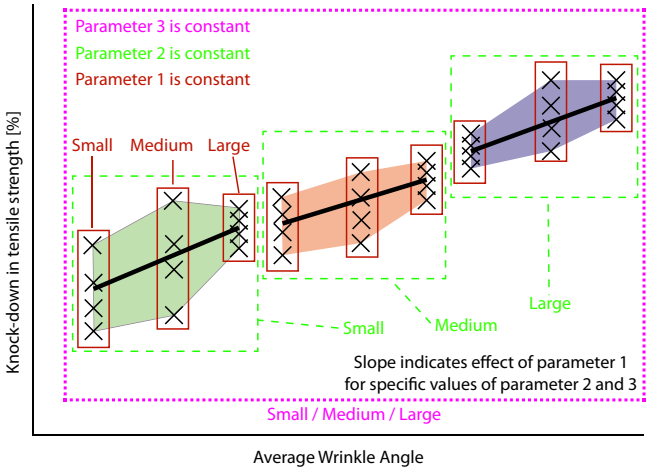

Fig. 9 Illustration of how the plots in the section are to be interpreted.

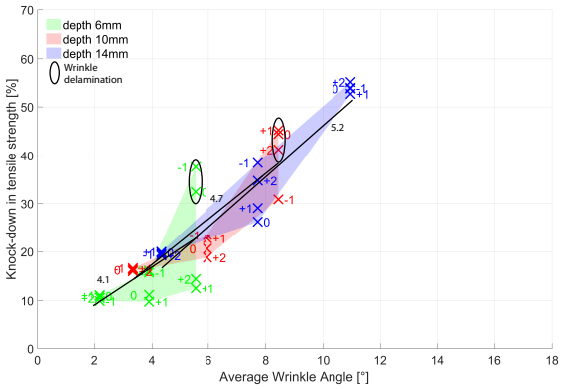

Fig. 10a Effect of the average wrinkle angle on the knock-down in tensile strength, with a **constant wash out degree of 1**. (The slope of the shaded areas indicate the **effect of the wrinkle angle**)

5.3 Depth and Wash Out Degree

The sensitivity of the knock-down to the depth is only slightly affected by the maximum wrinkle angle, meaning that a deeper wrinkle increases the knock-down approximately the same amount independent of the maximum wrinkle angle. This is indicated by the similar slopes in Fig. 11a, 11b, and 11c, respectively and

Table 2 Sensitivity of the knock-down to the maximum angle with combinations of wash out degrees (O) and depth (D). (results from Fig. 10a, 10b, and 10c)

O \ D	6mm	10mm	14mm
1	4.1	4.7	5.2
3	6.3	4.9	4.7
5	5.8	5.1	4.4

Table 3 Sensitivity of the knock-down to the depth with combinations of wash out degrees (O) and maximum angle (A). (results from Fig. 11a, 11b, and 11c)

O \ A	12°	21°	29°
1	4.2	4.9	5.5
3	2.4	2.1	2.8
5	0.9	0.6	2.2

Table 4 Sensitivity of the knock-down to the wash out degree with combinations of depth (D) and maximum angle (A). (results from Fig. 12a, 12b, and 12c)

D \ A	12°	21°	29°
6mm	5.4	15.3	7.7
10mm	3.0	6.8	4.6
14mm	0.7	5.0	2.1

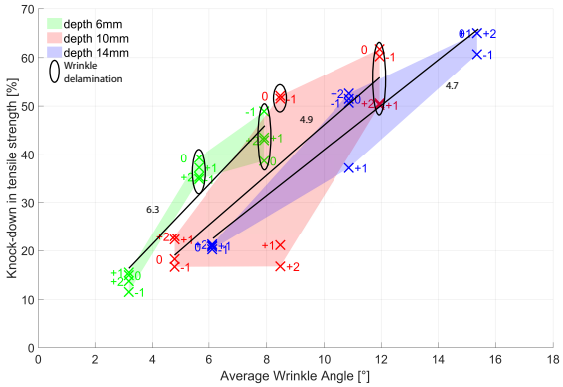

Fig. 10b Effect of the average wrinkle angle on the knock-down in tensile strength, with a **constant wash out degree of 3**. (The slope of the shaded areas indicate the **effect of the wrinkle angle**)

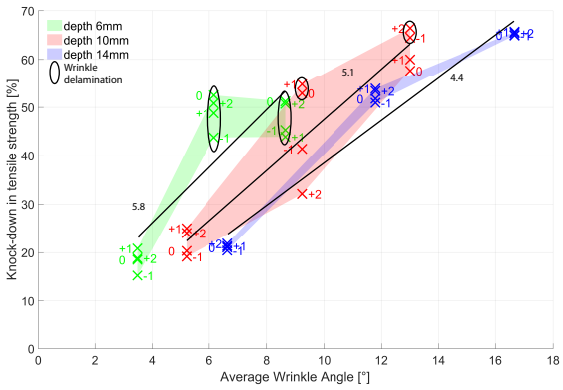

Fig. 10c Effect of the average wrinkle angle on the knock-down in tensile strength, with a **constant wash out degree of 5**. (The slope of the shaded areas indicate the **effect of the wrinkle angle**)

coefficients in Table 3. On the other hand, the sensitivity of the knock-down to the wash out degree is affected by the maximum wrinkle angle, meaning that an increase in wash out degree will cause different increases in knock-down for different maximum wrinkle angles. This is indicated by the different slopes in Fig. 12a, 12b, and 12c, respectively and coefficients in Table 4. It seems that medium maximum wrinkle angles are more sensitive to changes in the wash out degree than small and large maximum wrinkle angles. A possible reason for this is that the final delaminations associated with a small depth, a medium maximum wrinkle angle, and a medium to large wash out degree (the data points in the middle and to the right in the red area of Fig. 12a) are all wrinkle delaminations. The change in wash out degree severely changes the local wrinkle angle in the area where the delamination occurs.

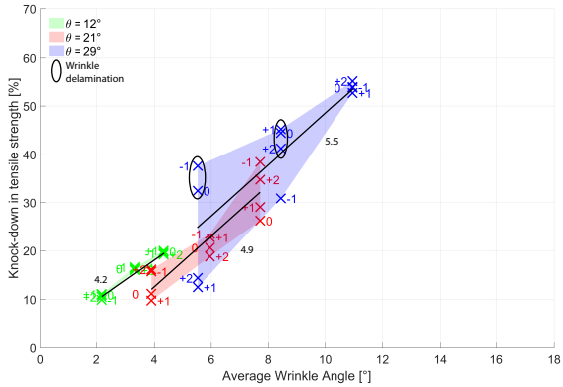

Fig. 11a Effect of the average wrinkle angle on the knock-down in tensile strength, with a **constant wash out degree of 1**. (The slope of the shaded areas indicate the **effect of the depth**)

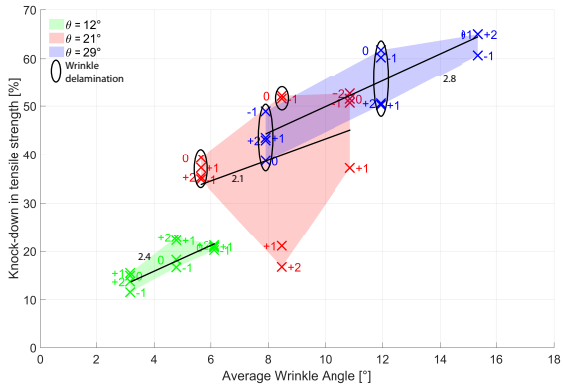

Fig. 11b Effect of the average wrinkle angle on the knock-down in tensile strength, with a **constant wash out degree of 3**. (The slope of the shaded areas indicate the **effect of the depth**)

Therefore, the knock-down is increased significantly while the average wrinkle angle is only increased marginally.

By considering the slopes of the shaded areas in Fig. 11a-c it is evident that the depth of the wrinkle becomes less important as the wash out degree increases. When the wash out degree is large, the depth has almost no influence on the knock-down for small and medium maximum wrinkle angles. The same goes for the wash out degree when the depth increases as shown in Fig. 12a-c. When the depth is large, the wash out degree has almost no influence on the knock-down for small maximum wrinkle angles.

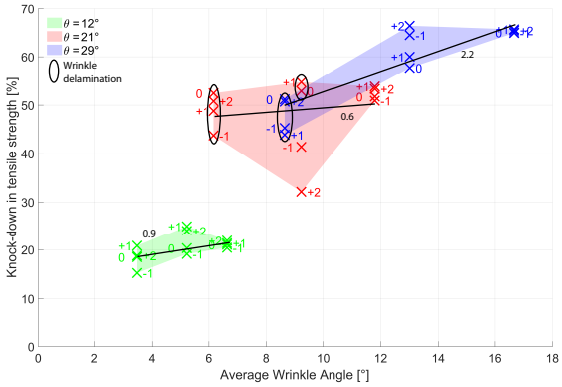

Fig. 11c Effect of the average wrinkle angle on the knock-down in tensile strength, with a **constant wash out degree of 5**. (The slope of the shaded areas indicate the **effect of the depth**)

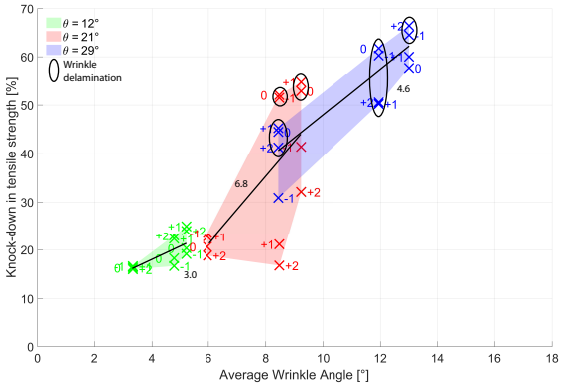

Fig. 12b Effect of the average wrinkle angle on the knock-down in tensile strength, with a **constant depth of 10mm**. (The slope of the shaded areas indicate the **effect of the wash out degree**)

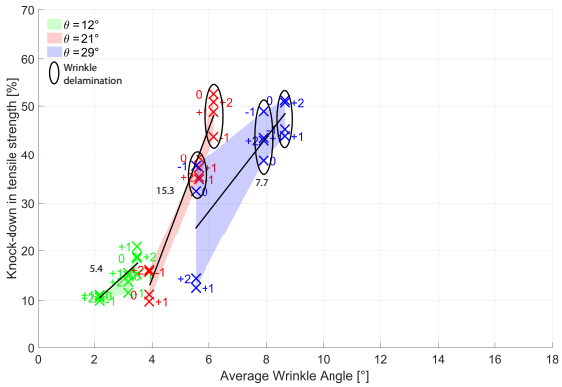

Fig. 12a Effect of the average wrinkle angle on the knock-down in tensile strength, with a **constant depth of 6mm**. (The slope of the shaded areas indicate the **effect of the wash out degree**)

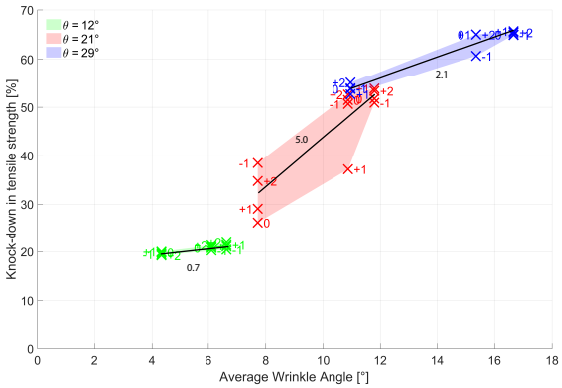

Fig. 12c Effect of the average wrinkle angle on the knock-down in tensile strength, with a **constant depth of 14mm**. (The slope of the shaded areas indicate the **effect of the wash out degree**)

5.4 Location

The location of the wrinkle has little effect on the load at final failure for wrinkles with small maximum wrinkle angle. However, the location has a significant effect in the mid-range of average wrinkle angles meaning wrinkles of medium maximum wrinkle angle with low to high depths, and wrinkles with high maximum wrinkle angles with low to medium depths. In this interval, the maximum wrinkle angles are medium or large, but the layers are not wavy all the way to the insert, meaning that a significant amount of delamination can occur at the wrinkle before final delamination either at the insert or away from the insert. For the large wrinkles with high depth, the location has almost no influence. For this case, the stress at the insert is increased significantly by the wrinkle, and delamination occurs here earlier than between two wrinkled plies. This indicates that the location only has an influence when delaminations can occur almost simultaneously at the insert and between two wrinkled plies. From the numbers next to the data points in Figures 11a to 12c it is not possible to detect any clear tendencies between the location of the wrinkle and the load at final failure. There is a slight indication that when the wrinkle is at +2mm the knock-down is reduced compared to the other locations. This is indicated by the data in Fig. 12b where a location of +2mm yields the lowest knock-down for a medium maximum wrinkle angle with any wash out degree and medium depth. This seems reasonable since the normal stress from the wrinkle is highly concentrated. Thus moving the wrinkle further away from the tip of the insert limits the interaction between the two.

6. Discussion

Fig. 13 is a combination of all the data points in Fig. 11a, 11b, and 11c. It is shown in the figure that there is a fairly good agreement between the average wrinkle angle and the knock-down in tensile strength for small and large average wrinkle angles. For the mid-range of average wrinkle angles there is a lot more scatter, and to determine the knock-down solely based on the average wrinkle angle in this region is futile. The knock-down ranges from 15% to 55% for average wrinkle angles from 6° to 10°. The figure also shows that small, medium, and large maximum wrinkle angles can cause a knock-down from 10 - 25%, 10 - 55%, and 12 - 66%, respectively by varying the depth, wash out, and location of the wrinkle. This means that the maximum wrinkle angle is controlling the possible minimum and maximum knock-down values, but the three other parameters are also important in determining the knock-down. The knock-down value changes $\approx$ 40% when varying the maximum wrinkle angle from 12° - 29° , which is very similar to the results reported in [8]. However, in this work there is a clear interaction with the depth and wash out degree, which was not reported in [8]. This indicates that the parameters are interacting more when the wrinkle is in close vicinity to the termination of a tapered beam.

All presented results from wrinkled sub-structures in the parametric study are numerical. A thorough comparison of numerical and experimental results for wrinkled sub-structures are presented in [13]

None of the studied parameters are by themselves enough to

determine the knock-down caused by the wrinkle. The average wrinkle angle can thus not be used on its own to determine the knock-down. Based on this, all the parameters must be identified for a given wrinkle in a tapered beam, and used as input in a numerical simulation to determine the knock-down caused by the wrinkle.

The parametric study shows that the maximum wrinkle angle is always important to measure accurately as 0.6mm in height for a 10mm long wrinkle can cause a difference in knock-down of up to 30%. Furthermore, the depth and wash out degree may be very impractical to measure, but their influence on the knock-down is non-negligible and these should be modelled with accuracy to achieve good results.

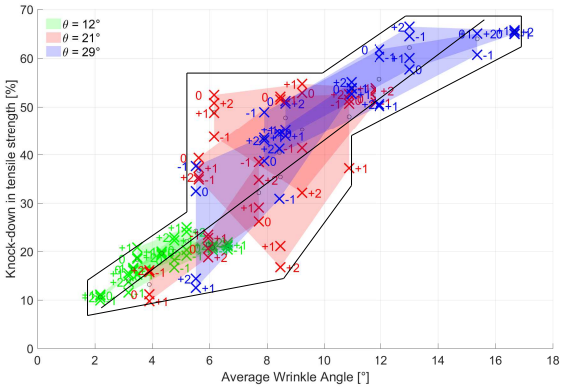

Fig. 13 All 108 data points from Fig. 11a, 11b, and 11c.

7. Conclusion

The interaction between pultruded tapered beam inserts and wrinkles of different severity has been investigated. A numerical parametric study with four parameters namely, maximum wrinkle angle, depth, location, and wash out degree has been performed. All four parameters influence the severity of the wrinkle, and they all have an impact on the load at final failure. The effect of the four parameters is highly interactive, meaning that the influence of one parameter is dependent on the size of the other parameters. The parameter that is least dependent on the others is the maximum wrinkle angle. The effect of the maximum wrinkle angle on the load at final failure is almost constant w.r.t. depth and wash out degree. The importance of the other three parameters is assessed as follows:

Small maximum wrinkle angle

- The depth and the wash out degree of the wrinkle are very important features of small wrinkles, unless one of them is large, in that case the other parameter has almost no influence on the knock-down, as shown in Fig. 11c and 12c. The location has almost no effect on small wrinkles.

Medium maximum wrinkle angle

- The wash out degree has the most influence on the knock-down for medium wrinkles. The influence decreases when the depth is increased. The depth has some influence on the knock-down when the wash out degree is low, but as it increases, the influence of the depth vanishes. This is shown in Table 3 and 4. The location can be important if the average wrinkle angle is between 6° - 11°. In this region, there is a possibility that the final delamination can initiate away from the insert if the location of the wrinkle is changed. This can cause a significantly different knock-down.

Large maximum wrinkle angle

- The wash out degree and the depth can be equally influential on the knock-down. When one of them is low, the other is important, and vice versa. Both parameters have limited influence when the other is large as shown in Table 3 and 4. The location can be important if the average wrinkle angle is between 6° - 13°, but only if the depth is low to medium.

Acknowledgement

This work is part of a Ph.D. project at the Department of Materials and Production at Aalborg University, Denmark. Most of the numerical modelling was conducted during a research stay of the corresponding author at Bristol Composites Institute (ACCIS) at the University of Bristol. The work is supported by the Innovation Fund Denmark project OPTI_MADE_BLADE, grant no. 75-2014-3. This support is gratefully acknowledged.

References

[1] K. B. Katnam, A. J. Comer, D. Roy, L. F. M. Da Silva, and T. M. Young, "Composite repair in wind turbine blades: An overview," *Journal of Adhesion*, vol. 91, pp. 113–139, 2015.

[2] B. Hayman, C. Berggreen, and R. Pettersson, "The Effect of Face Sheet Wrinkle Defects on the Strength of FRP Sandwich Structures," *Journal of Sandwich Structures and Materials*, vol. 9, no. 4, pp. 377–404, 2007.

[3] S. Mukhopadhyay, M. I. Jones, and S. R. Hallett, "Compressive failure of laminates containing an embedded wrinkle; experimental and numerical study," *Composites Part A: Applied Science and Manufacturing*, vol. 73, pp. 132–142, 2015. [Online]. Available: http://www.sciencedirect.com/science/article/pii/S1359835X15001013

[4] S. Mukhopadhyay, M. I. Jones, and S. R. Hallett, "Tensile failure of laminates containing an embedded wrinkle; numerical and experimental study," *Composites Part A: Applied Science and Manufacturing*, vol. 77, pp. 219–228, 2015. [Online]. Available: https://doi.org/10.1016/j.compositesa.2015.07.007

[5] M. Leong, L. C. T. Overgaard, O. T. Thomsen, E. Lund, and I. M. Daniel, "Investigation of failure mechanisms in GFRP sandwich structures with face sheet wrinkle defects used for wind turbine blades," *Composite Structures*, vol. 94, no. 2, pp. 768–778, 2012. [Online]. Available: http://dx.doi.org/10.1016/j.compstruct.2011.09.012

[6] J. W. Nelson, T. W. Riddle, and D. S. Cairns, "Effects of defects in composite wind turbine blades – Part 1: Characterization and mechanical testing," *Wind Energy Science Discussions*, vol. 2, pp. 641–652, apr 2017. [Online]. Available: https://www.wind-energ-sci.net/2/641/2017/

[7] L. D. Bloom, J. Wang, and K. D. Potter, "Damage progression and defect sensitivity: An experimental study of representative wrinkles in tension," *Composites Part B: Engineering*, vol. 45, no. 1, pp. 449–458, 2013. [Online]. Available: http://www.sciencedirect.com/science/article/pii/S1359836812003472

[8] N. Xie, R. A. Smith, S. Mukhopadhyay, and S. R. Hallett, "A numerical study on the influence of composite wrinkle defect geometry on compressive strength," *Materials and Design*, vol. 140, pp. 7–20, 2018. [Online]. Available: https://doi.org/10.1016/j.matdes.2017.11.034

[9] P. Agastra, D. D. Samborsky, and J. F. Mandell, "Fatigue Resistance of Fiberglass Laminates at Thick Material Transitions," in *2009 AIAA SDM Wind Energy Special Session*. Palm Springs: AIAA-2009-2411, 2009, pp. 1–23. [Online]. Available: http://arc.aiaa.org/doi/abs/10.2514/6.2009-2411

[10] K. W. Gan, G. Allegri, and S. R. Hallett, "A simplified layered beam approach for predicting ply drop delamination in thick composite laminates," *Materials and Design*, vol. 108, pp. 570–580, 2016. [Online]. Available: http://dx.doi.org/10.1016/j.matdes.2016.06.105

[11] G. B. Murri, "Influence of Ply Waviness on Fatigue Life of Tapered Composite Flexbeam Laminates," NASA, Tech. Rep. December, 1999. [Online]. Available: http://hdl.handle.net/2060/20000017962

[12] D. O. Adams and M. W. Hyer, "Effects of Layer Waviness on the Compression Strength of Thermoplastic Composite Laminates," *Journal of Reinforced Plastics and Composites*, vol. 12, no. 4, pp. 414–429, 1993.

[13] J. J. Bender, S. R. Hallett, and E. Lindgaard, “Investigation of the Effect of Wrinkle Features on Wind Turbine Blade Sub-structure Strength,” *Submitted to Composite Structures*, 2018.
[14] J. W. Nelson, T. W. Riddle, and D. S. Cairns, “Effects of Defects in Composite Wind Turbine Blades : Round 2,” Sandia National Laboratories, Tech. Rep. September, 2012. [Online]. Available: http://prod.sandia.gov/techlib/access-control.cgi/2012/128111.pdf